Evaluating the prognostic potential of the ki67 index and tumor infiltrating lymphocytes in olfactory neuroblastoma

Marion Classe, Alice Burgess, Sophie El Zein, Michel Wassef, Philippe Herman, Geoffrey Mortuaire, Xavier Leroy, Gabriel G. Malouf, Benjamin Verillaud

Histopathology

Histopathology 2019, **75**, 853–864. DOI: 10.1111/his.13954

Evaluating the prognostic potential of the Ki67 proliferation index and tumour-infiltrating lymphocytes in olfactory neuroblastoma

Marion Classe,[1] Alice Burgess,[2,3] Sophie El Zein,[4] Michel Wassef,[4] Philippe Herman,[2,3] Geoffrey Mortuaire,[5] Xavier Leroy,[6] Gabriel G Malouf[7] & Benjamin Verillaud[2,3]

[1]*Department of Pathology, Institut Gustave Roussy, Villejuif,* [2]*Department of Otolaryngology – Head and Neck Surgery, Assistance Publique–Hopitaux de Paris, Lariboisière Hospital,* [3]*Faculty of Medicine, Paris Diderot University,* [4]*Department of Pathology, Assistance Publique–Hopitaux de Paris, Lariboisière Hospital, Paris,* [5]*Department of Otolaryngology – Head and Neck Surgery, University Hospital and Lille 2 Faculty of Medicine,* [6]*Department of Pathology, University Hospital and Lille 2 Faculty of Medicine, Lille, and* [7]*Department of Medical Oncology, Hôpitaux Universtiaires de Strasbourg, Institut de Génomique et de Biologie Moléculaire et Cellulaire, Strasbourg, France*

Date of submission 13 May 2018
Accepted for publication 11 July 2019
Published online *Article Accepted* 15 July 2019

Classe M, Burgess A, El Zein S, Wassef M, Herman P, Mortuaire G, Leroy X, Malouf G G & Verillaud B (2019) *Histopathology* **75**, 853–864. https://doi.org/10.1111/his.13954

Evaluating the prognostic potential of the Ki67 proliferation index and tumour-infiltrating lymphocytes in olfactory neuroblastoma

Aims: Olfactory neuroblastomas (ONBs) are rare malignant tumours that arise in the nasal vault. To date, the Hyams grade remains the only widely used histological grading system. However, it is based only on morphological criteria, and has not been updated since 1988. The objective of this study was to explore the prognostic potential of the Ki67 proliferation index (PI) and tumour-infiltrating lymphocytes (TILs) in ONB.
Methods and results: A retrospective study was conducted on a bicentric series of 45 cases. The Ki67 PI was determined by counting at least 1000 nuclei on whole slides. TILs were evaluated with CD20, CD4 and CD8 immunohistochemical markers on whole slides. In this series, Hyams grades I, II, III and IV accounted for 13.4%, 44.4%, 20% and 22.2% of all cases, respectively. The Ki67 PI ranged from 1 to 93; the Ki67 PI was significantly higher in Hyams grade III–IV ONBs than in Hyams grade I–II ONBs ($P < 0.0001$). A Ki67 PI of ≥25 was associated with poorer survival ($P = 0.02$). TILs were present in both stromal and intratumoral compartments, but were located predominantly in the stromal component of the tumour. The numbers of intratumoral CD8+ cells/mm^2 and CD4+ cells/mm^2 were greater in high-grade ONBs than in low-grade ONBs ($P = 0.0015$ and $P = 0.043$, respectively). The numbers of T cells/mm^2 and B cells/mm^2 were not associated with survival, but a CD4/CD8 ratio of >2 was significantly associated with shorter survival ($P = 0.04$).
Conclusion: Our findings suggest that the Ki67 PI and TILs could be used as prognostic markers, as a potential alternative to the Hyams grade.

Keywords: aesthesioneuroblastoma, Ki67, olfactory neuroblastoma, tumour-infiltrating lymphocytes

Introduction

Olfactory neuroblastoma (ONB), also known as aesthesioneuroblastoma, is a rare malignant tumour arising in the nasal vault. It accounts for 3% of all sinonasal tumours,[1] with an annual incidence of four cases per 10 million people.[2] It is thought to develop

Address for correspondence: M Classe, Department of Pathology, Institut Gustave Roussy, 114 rue Edouard Vaillant, 94805 Villejuif Cedex, France. e-mail: marionclasse@hotmail.fr
M.C. and A.B. contributed equally to this work.

in the olfactory neuroepithelium, but its exact cell of origin has not yet been confirmed.[3] ONB can occur at any age (2–90 years), and peaks in the fourth and fifth decades of life.[4] A slight sex predilection has been described, and a male/female ratio of 1.2:1 was recently reported,[1] but no risk factor has been identified. Its clinical presentation has no specificity, and, like other sinonasal tumours, ONBs are often responsible for nasal obstruction, epistaxis, and, sometimes, anosmia. The histological features of these tumours are now well described: ONBs are among the 'small round blue cell tumours',[5,6] but their biology is not fully understood. ONBs show a neuroendocrine immunohistochemical profile, resulting in them being reported in many studies focusing on the neuroendocrine tumours of the sinonasal region.[4,7] ONBs are classified by the World Health Organization, in the chapter dedicated to neuroectodermal/melanotic tumours, as 'round blue cell' tumours.[1] There is no consensus on the best treatment strategy for ONB. Low-grade ONBs are usually treated with surgery, followed by radiotherapy,[8] but high-grade and clinically advanced ONBs can be difficult to manage.[3] In this context, clinical and pathological grading systems are key tools in the discussion of treatment options. Several staging systems have been described,[9,10] the most popular being the Kadish system (first described in 1976, and modified by Morita *et al.* in 1993[11]). In contrast, there are very few histological grading systems; in general, there is a lack of histological prognostic markers for ONB. To date, the only widely used histological grading system is the Hyams grading system. It was established in 1988, and has not been updated since then.[12] Although it has been extensively used over the past 30 years,[3,13–15] several authors have underlined its limitations and drawbacks.[12,14] First, it is based on morphological criteria and its reproducibility is therefore questionable. Secondly, it does not integrate any of the immunohistochemical features of tumours, and finally, it does not address the issue of the tumour microenvironment. Among the many potential markers for ONB, the Ki67 proliferation index (PI) is of particular interest. The Ki67 PI is reproducible and is widely used in neuroendocrine tumours.[16] Its prognostic value has been evaluated for ONBs in several studies, but no prognostic threshold could be determined, possibly because of a lack of power (limited number of patients).[17,18]

With regard to the tumour microenvironment, the major role of immune responses against cancer cells is now well recognised.[19–21] In particular, it has been shown that tumour-infiltrating lymphocytes (TILs) play a specific role in immune responses in many cancers, including head and neck cancers,[22,23] and may be used as both prognostic and therapeutic tools. To our knowledge, their role in ONB has never been studied.

The objective of our study was to assess, on the basis of a bicentric retrospective series of 45 patients: (i) the Ki67 PI and TILs in ONB; (ii) the correlation between the Ki67 PI, TILs, and the Hyams grade; and (iii) the prognostic value of the Ki67 PI and TILs.

Materials and methods

CASE SELECTION

All cases of olfactory neuroblastoma treated between January 2004 and December 2015 at two university hospitals (Lariboisière Hospital, Assistance Publique–Hôpitaux de Paris, and Lille University Hospital) were retrospectively retrieved from the databases of the pathology departments. The diagnoses were confirmed in all of the cases by a senior head and neck pathologist (M.W.). The immunohistochemical panel used to confirm the diagnosis was chromogranin A, synaptophysin, neural cell adhesion molecule (CD56), S100, and cytokeratin (CK) AE1/AE3. If CK AE1/AE3 was quite diffusely positive (more than scarce positive cells), the diagnosis was considered to be positive if two neuroendocrine markers were positive in >1% of tumour cells and if at least focal S100-positive sustentacular cells were observed. Patients for whom no clinical data were available or those for whom no biopsy/specimen was available for immunohistochemical analysis were excluded from the study. The study was approved by the local ethics committee.

CLINICOPATHOLOGICAL ANALYSIS

When both the biopsy specimen and the surgical specimen were available, biopsy was favoured in cases with neoadjuvant therapy. When several paraffin blocks were available for the same tumour, the most representative block was selected for immunohistochemical analysis. Cases in which the fixative was not formalin, and decalcification had been applied, were excluded, to avoid immunohistochemical issues. Clinical data were collected from patients' medical files. The data collected included sex, age at the time of diagnosis, location and local extension of the tumour, Kadish stage, Dulguerov stage, treatment modalities, time to progression, and time to death.

KI67 AND TIL QUANTIFICATION

All of the immunohistochemical analyses were performed on serial freshly cut 4-μm sections of the selected block. Stains were obtained with a Ventana Benchmark (Ventana Medical Systems, Tucson, AZ, USA) automated method (the protocols are summarized in Table S1). Ki67 was studied by the use of clone MIB1 (Dako, Agilent, Santa Clara, CA, USA). To characterise the TILs, whole sections were stained for CD20 (clone L26; Dako), CD4 (clone SP35; Ventana Medical Systems, Tucson, AZ, USA), and CD8 (clone 144B; Dako). CD20 was used to identify B cells, and CD4 and CD8 were used to identify the subpopulations of T cells.

Quantification of the Ki67 PI was performed by counting hotspots, with IMAGEJ software. A minimum of 1000 nuclei were counted to determine the percentage of positive nuclei. To confirm the relevance of the Ki67 PI, it was compared with a mitotic count for 10 high-power fields (2.5 mm^2). For quantification of TILs, slides were digitalised with an Aperio AT2 slide scanner (Leica Biosystems, Wetzlar, Germany). On digitalised slides, regions of interest (ROIs) (hotspots) were identified at low magnification; then, five fields of 0.2 μm^2 were delimited with the Aperio IMAGESCOPE software (Leica Biosystems). Lymphocytes were then counted in each ROI with the IMAGESCOPE counting tool. Lymphocytes were counted, blinded to the clinical data, within the stromal area of the tumour and within the tumour lobules themselves. CD4+ cells showing macrophage-like features were excluded.

STATISTICS

Statistical analyses were performed with Fisher's exact test for categorical variables and the Mann–Whitney *U*-test for continuous variables (GraphPad Software, La Jolla, CA, USA). The correlation between two continuous parameters was evaluated by use of the Pearson coefficient when the distribution was normal, and by use of the Spearman coefficient otherwise. The cumulative survival time was calculated with the Kaplan–Meier method, and analysed with a log-rank test (GraphPad Software). A *P*-value of <0.05 was considered to be significant.

Results

CLINICOPATHOLOGICAL FEATURES

The main clinicopathological data are summarised in Table 1. Forty-five patients were included. The mean age was 52.3 years (range: 13–88 years). No peak of incidence was observed. The male/female ratio was 0:8. None of the patients had a history of carcinoma. There was a predominance of the Kadish C (66.7%) and Dulguerov T4 (42.2%) stages. The Hyams grade distribution showed a predominance of grade II cases (42.2%), followed by approximately the same proportion of grade III (26.7%) and VI (22.2%) cases, and a few grade I (8.9%) cases. Surgery was performed in 84.5% of the cases. Of these, 29% had received neoadjuvant chemotherapy and 69% had received adjuvant radiotherapy. Fifteen per cent of the patients were treated with surgery alone, and 11% were treated only with radiotherapy and/or chemotherapy, without surgery. The mean follow-up was 46 months (range: 1–191 months), and one patient (2.2%) were lost to follow-up. Recurrence was observed in eight cases, either locally ($n = 4$: orbit and cerebral falx) or at distant locations ($n = 5$: cervical lymph node, vertebrae, and leptomeninges). The mean delay for recurrence was 57 months. At the last follow-up, six patients (13.3%) had died of the disease, one patient (2.2%) had died of radiation-induced osteosarcoma, five patients (11.1%) were alive with disease, and 31 patients (68.9%) were alive and free of disease.

KI67 PI

The Ki67 PI distribution, according to the Hyams grade, is summarised in Table 2. An example of Ki67 staining in Hyams grade I–IV tumours is shown in Figure 1. The Ki67 PI was significantly lower in Hyams I–II ONBs than in Hyams III–IV ONBs ($P < 0.0001$) (Figure 2A). A receiver operating characteristic curve showed that the best compromise between sensitivity and specificity for the Ki67 PI was a threshold of <22 (Figure 2B; Table S2) with a likelihood ratio of 1.5, and that the specificity decreased when the threshold value of 27 was reached. As the highest Ki67 value of Hyams I–II ONBs was 25 (Table 2), the threshold for further analyses was then set at 25. A Ki67 PI of ≥25 was associated with shorter survival ($P = 0.017$; Figure 2C). To validate the results obtained with the Ki67 PI, a mitotic count distribution was performed as described in Materials and methods. The results are summarised in Table S3. A strong correlation was observed between mitotic count/2.5 mm^2 and the Ki67 PI ($P < 0.0001$) (Figure S1).

TUMOUR-INFILTRATING LYMPHOCYTES

The distribution of TILs is summarised in Table 3 and Figure 3. TILs were observed in both stromal and intratumoral compartments, but they were located

Table 1. Patient characteristics

Characteristics	All cases	Hyams I–II	Hyams III–IV	Ki67 PI < 25	Ki67 PI ≥ 25	CD4/CD8 < 2	CD4/CD8> 2
No. of patients available	45	23	22	22	21	33	12
Age (years)							
Median	52	51	51.5	47.5	58	53	47.5
Range	13–88	13–78	16–88	13–78	16–88	13–88	16–80
Sex, *n* (%)							
Male	24 (53.3)	8 (34.7)	16 (72.7)	10 (45.5)	11 (52.4)	16 (48.5)	8 (66.7)
Female	21 (46.7)	15 (65.3)	6 (27.3)	12 (54.5)	7 (47.6)	17 (51.5)	4 (33.3)
Modified Kadish stage, *n* (%)							
A	1 (2.2)	1 (4.3)	0 (0)	1 (4.5)	0 (0)	1 (3.03)	0 (0)
B	8 (17.8)	6 (26.2)	2 (9)	5 (22.7)	2 (9.5)	7 (21.2)	1 (8.3)
C	30 (66.7)	14 (60.9)	16 (72.7)	15 (68.3)	14 (66.7)	21 (63.6)	9 (75)
D	4 (8.9)	1 (4.3)	3 (13.7)	1 (4.5)	3 (14.3)	2 (6.1)	2 (16.7)
Unknown	2 (4.4)	1 (4.3)	1 (4.6)	0 (0)	2 (9.5)	2 (6.1)	0 (0)
Dulguerov T stage, *n* (%)							
T1	5 (11.1)	4 (17.4)	1 (4.5)	3 (13.7)	1 (4.8)	5 (15.1)	0 (0)
T2	7 (15.6)	4 (17.4)	3 (13.7)	4 (18.2)	3 (14.3)	6 (18.2)	1 (8.3)
T3	12 (26.7)	5 (21.7)	7 (31.8)	6 (27.3)	6 (28.6)	9 (27.3)	3 (25)
T4	19 (42.2)	9 (39.2)	10 (45.5)	9 (40.8)	9 (42.9)	11 (33.3)	8 (66.7)
Unknown	2 (4.4)	1 (4.3)	1 (4.5)	0 (0)	2 (9.4)	2 (6.1)	0 (0)
Surgery, *n* (%)							
Yes, combined with radiotherapy	31 (68.9)	18 (78.3)	13 (59.1)	17 (77.4)	13 (61.9)	22 (66.7)	9 (75)
Yes, alone	7 (15.6)	3 (13.1)	4 (18.2)	3 (13.6)	3 (14.3)	5 (15.1)	2 (16.7)
No, chemotherapy and/or radiotherapy alone	5 (11.1)	0 (0)	5 (22.7)	0 (0)	5 (23.8)	4 (12.1)	1 (8.3)
Unknown	2 (4.4)	2 (8.6)	0	2 (9)	0 (0)	2 (6.1)	0 (0)
Surgical margins, *n* (%)							
R0	19 (42.2)	10 (43.5)	9 (40.9)	11 (50)	8 (38.1)	16 (48.5)	3 (25)
R1	11 (24.5)	6 (26.1)	5 (22.7)	5 (22.7)	5 (23.8)	4 (12.1)	7 (58.3)
Rx	15 (33.3)	7 (30.4)	8 (36.4)	6 (27.3)	8 (38.1)	13 (39.4)	2 (16.7)
Hyams grade, *n* (%)							
I	4 (8.9)	4 (17.4)	0 (0)	3 (13.6)	0 (0)	4 (12.1)	0 (0)
II	19 (42.2)	19 (82.6)	0 (0)	16 (72.8)	2 (9.4)	15 (45.4)	4 (33.3)
III	12 (26.7)	0 (0)	12 (54.5)	3 (13.6)	9 (42.9)	7 (21.2)	5 (41.7)
IV	10 (22.2)	0 (0)	10 (45.5)	0 (0)	10 (47.7)	7 (21.2)	3 (25)

Table 1. *(Continued)*

Characteristics	All cases	Hyams I–II	Hyams III–IV	Ki67 PI < 25	Ki67 PI ≥ 25	CD4/CD8 < 2	CD4/CD8> 2
Follow-up (months)							
Mean	46.4	48.1	44.6	41	44	43	37.5
Range	1–191	3–182	1–191	1–94	1–191	1–191	2–94
Recurrence, *n* (%)							
No	30 (66.7)	17 (73.9)	13 (59.1)	18 (81.8)	11 (52.4)	24 (72.7)	6 (50)
Yes, local	4 (8.9)	3 (13.1)	1 (4.5)	2 (9.2)	3 (14.3)	3 (9.1)	1 (8.3)
Yes, distant	5 (11.1)	2 (8.7)	3 (13.7)	1 (4.5)	3 (14.3)	1 (3)	4 (33.3)
Unknown	6 (13.3)	1 (4.3)	5 (22.7)	1 (4.5)	4 (19)	5 (15.1)	1 (8.3)
Status, *n* (%)							
Alive with no evidence of disease	31 (68.9)	16 (69.6)	15 (68.2)	18 (81.8)	12 (57.1)	25 (75.8)	6 (50)
Alive with disease	5 (11.1)	4 (17.4)	1 (4.5)	3 (13.7)	2 (9.5)	3 (9.1)	2 (16.7)
Dead of disease	6	1 (4.3)	5 (22.6)	0 (0)	6 (28.6)	2 (6.1)	4 (33.3)
Dead from another cause	2	1 (4.3)	1 (4.5)	1 (4.5)	1 (4.8)	2 (6.1)	0 (0)
Unknown	1 (2.2)	1 (4.3)	0 (0)	0 (0)	0 (0)	1 (3)	0 (0)

PI, Proliferation index.

predominantly in the stromal component of the tumour, and rarely infiltrated the tumour cell nests. The median stromal TIL number was 562, and the median intratumoral TIL number was 35, with the difference being highly significant ($P < 0.0001$; Figure 3A). T cells were more abundant than B cells ($P < 0.0001$; Figure 3B). The total number of T cells varied from 77 to 4114/mm^2 (median: 520). Among T cells, CD4+ cells were slightly more abundant than CD8+ cells ($P = 0.6$; Figure 3C). Both CD4+ and CD8+ cells were predominantly found in the stromal compartment ($P < 0.0001$; Figure 3D,E). Within the stromal and intratumoral compartments, the numbers of CD4+ cells/mm^2 and CD8+ cells/mm^2 were not significantly different ($P = 0.7$). B cells (CD20+ cells) were also found predominantly in the stromal compartment of the tumour, and their number varied from 163 to 1308/mm^2 (median: 79/mm^2) ($P < 0.0001$; Figure 3F). We then assessed the association between the distribution of TILs and Hyams grade. Examples of TILs in low-grade and high-grade ONBs are shown in Figure 4A–D. The numbers of intratumoral CD8+ cells/mm^2 and CD4+ cells/mm^2 were greater in Hyams III–IV ONBs than in Hyams I–II ONBs ($P = 0.0015$ and $P = 0.043$, respectively) (Table 4; Figure 5A,B). The survival data were used to further investigate the prognostic significance of TIL infiltration. The distribution of TILs did not follow a normal distribution (Figure S2): the TIL variables were therefore classified according to the quartiles. Neither the numbers of T cells/mm^2 (CD4+ or CD8+) nor the number of B cells/mm^2 were associated with

Table 2. Distribution of the Ki67 proliferation index between the four Hyams categories

Hyams	Minimum	Maximum	Mean	Median	Standard deviation	1st quartile	3rd quartile
I	2	10	5.4	4.3	3.68	2.4	9.5
II	1	25	13.3	11.9	8.13	8.4	20
III	8	90	44.7	51	27.64	17.5	66
IV	31	93	71.4	81.5	20.75	57	88

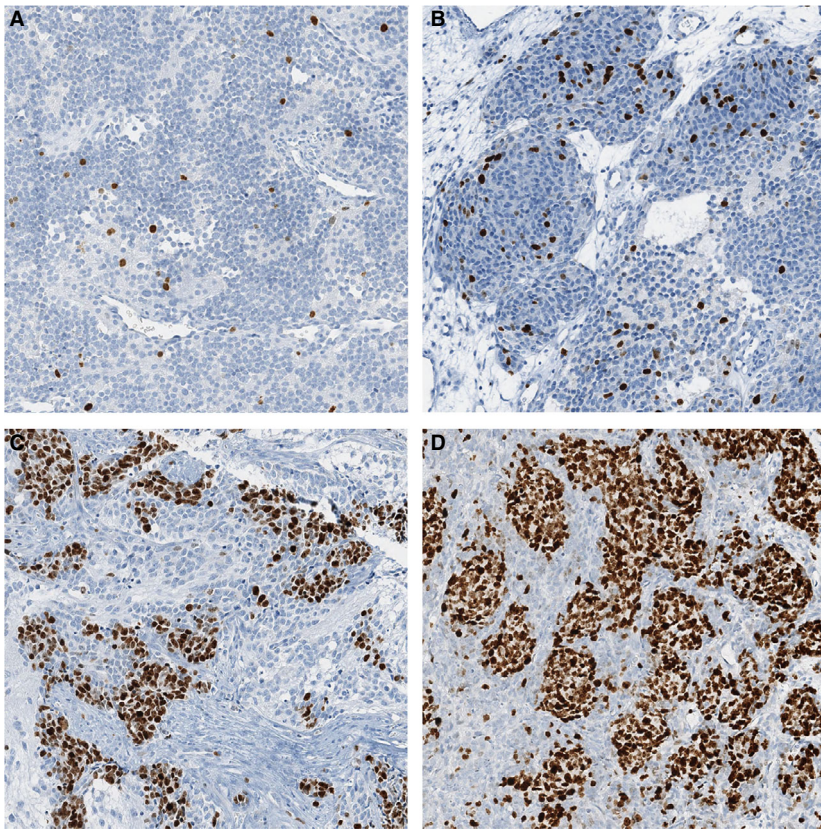

Figure 1. Examples of the Ki67 proliferation index (PI) in the four Hyams categories. **A**, Grade I olfactory neuroblastoma (ONB), Ki67 PI = 2.5. **B**, Grade II ONB, Ki67 PI = 11. **C**, Grade III ONB, Ki67 PI = 55. **D**, Grade IV ONB, Ki67 PI = 89.

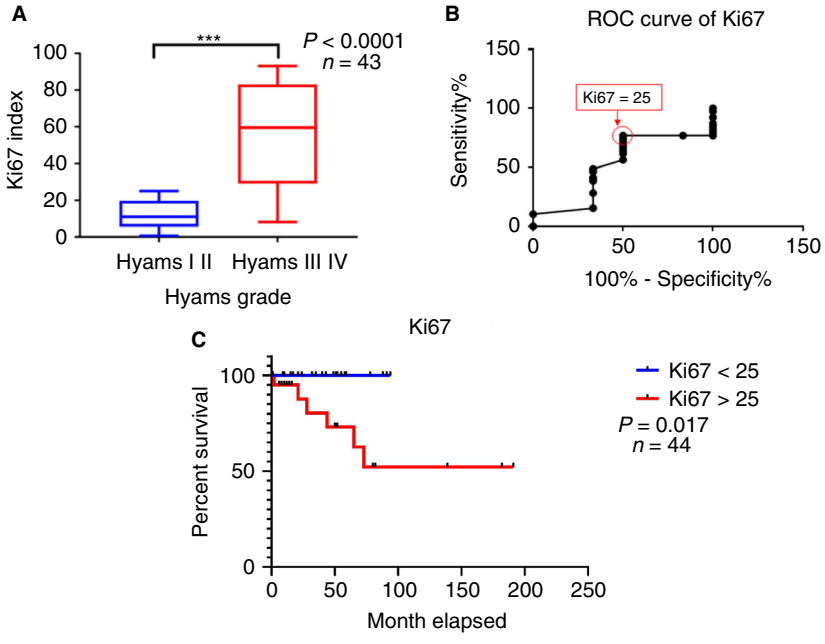

Figure 2. Correlation of the Ki67 proliferation index (PI) with the Hyams grade, and the related survival curve. **A**, Boxplot showing that the Ki67 PI was significantly lower in Hyams I–II olfactory neuroblastomas (ONBs) than in Hyams III–IV ONBs. **B**, Receiver operating characteristic curve for the Ki67 PI. **C**, Overall survival, according to the Ki67 PI, with 25 as a threshold; the Ki67 PI was not available for two patients, $n = 43$.

survival, but a CD4/CD8 ratio of >2 was significantly associated with shorter survival ($P = 0.04$; Figure 5C). Moreover, the number of intratumoral CD8+ and CD4+ cells was correlated with the Ki67 PI ($P = 0.03$ and $P = 0.04$, respectively) and mitotic count ($P = 0.0003$ and $P = 0.05$, respectively) (Table S4).

Table 3. Distribution of tumour-infiltrating lymphocytes (TILs) between the stromal and intraepithelial compartments

	Minimum	Maximum	Mean	Median	Standard deviation	1st quartile	3rd quartile
Stromal CD20+ TILs/mm^2	5	1302	155	79	218	22	208
Intraepithelial CD20+ TILs/mm^2	0	133	7	0	22	0	4
Stromal CD4+ TILs/mm^2	37	2972	459	224	621	105	452
Intraepithelial CD4+ TILs/mm^2	0	415	56	19	85	7	64
Stromal CD8+ TILs/mm^2	21	2096	315	210	362	137	270
Intraepithelial CD8+ TILs/mm^2	0	864	59	11	156	3	45
Global CD20+ TILs/mm^2	5	1308	163	79	223	22	236
Global CD4+ TILs/mm^2	37	3120	515	301	654	132	505
Global CD8+ TILs/mm^2	21	2960	374	227	490	150	340

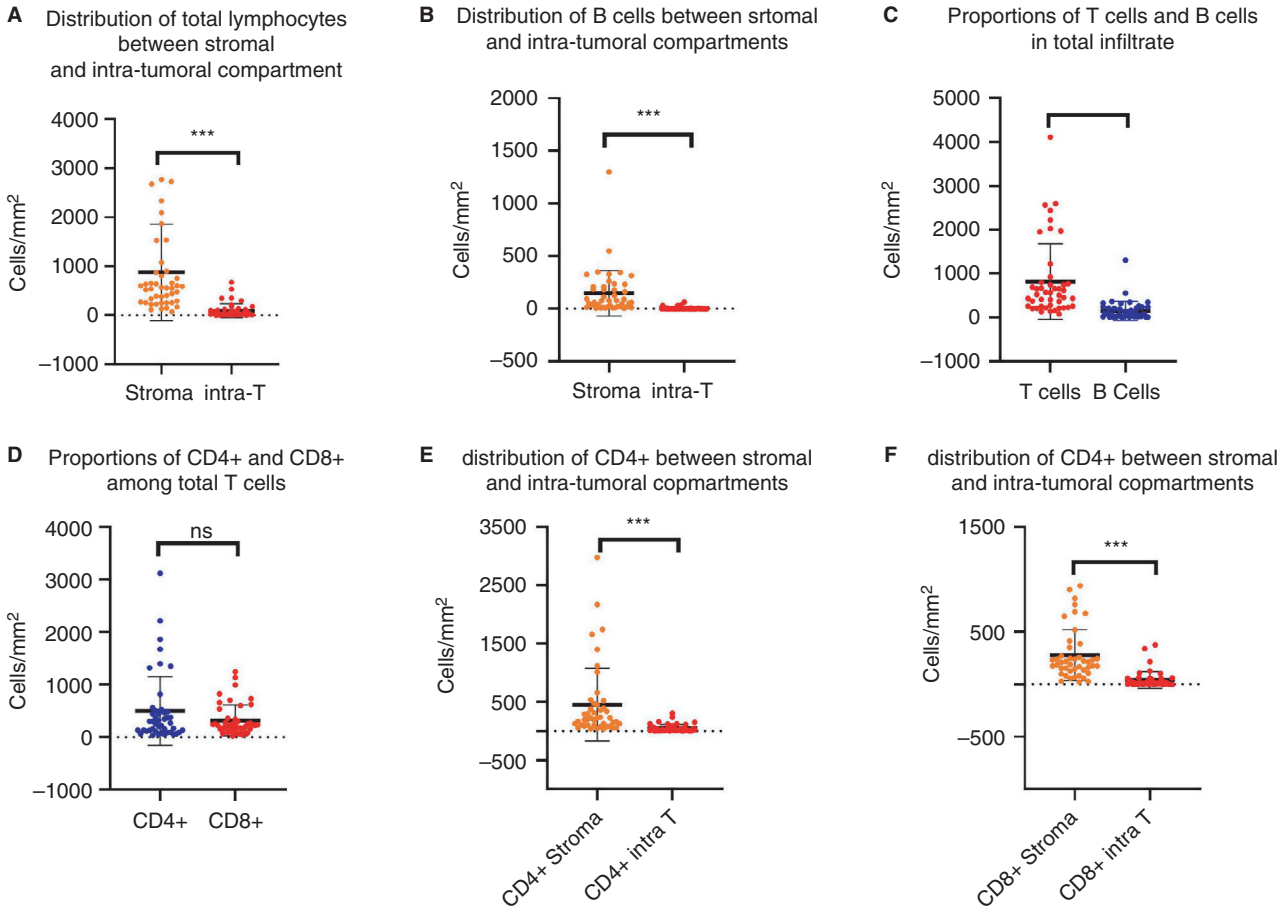

Figure 3. Scatter plots showing the distribution of tumour-infiltrating lymphocytes (TILs) in olfactory neuroblastomas. The error bars represent the mean and the standard deviation. **A**, Proportions of total TILs (CD8, CD4, and CD20) in intratumoral and stromal compartments. **B**, Proportions of T cells (CD4 and CD8) and B cells (CD20) among TILs. **C**, Proportions of total CD4+ cells and total CD8+ cells among TILs. **D**, Distribution of CD8+ cells between stromal and intratumoral compartments. **E**, Distribution of CD4+ cells between stromal and intratumoral compartments. **F**, Distribution of B cells (CD20) between stromal and intratumoral compartments. [Colour figure can be viewed at wileyonlinelibrary.com]

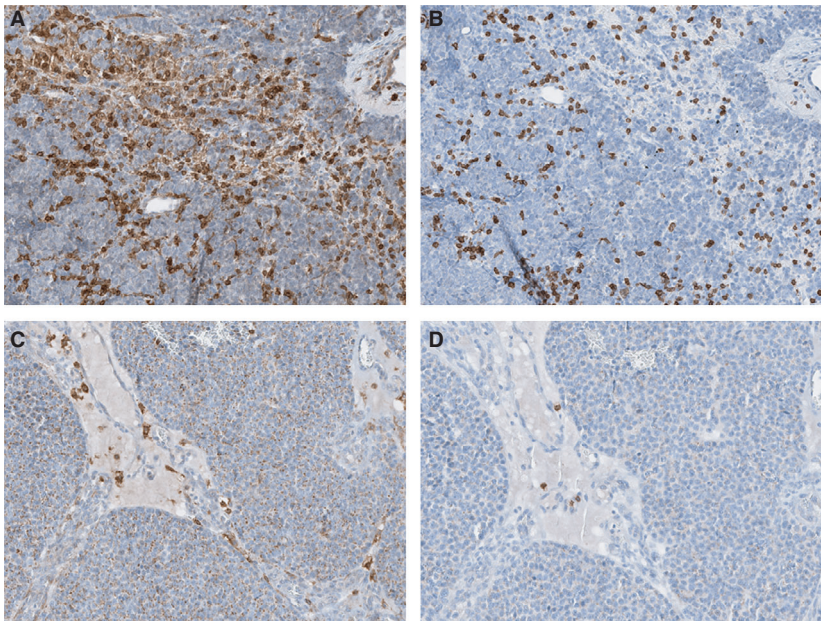

Figure 4. Immunohistochemical examples of tumour-infiltrating lymphocytes (TILs) in low-grade and high-grade olfactory neuroblastomas (ONBs). **A**,**B**, High-grade ONB highly infiltrated by TILs, with lymphocytes penetrating the tumour nests. **A**, CD4 staining. **B**, CD8 staining. **C**,**D**, Example of a low-grade ONB poorly infiltrated by CD4+ cells (**C**) and CD8+ cells (**D**). [Colour figure can be viewed at wileyonlinelibrary.com]

The number of intratumoral CD8+ T cells was higher in cases with a Ki67 PI of ≥25 ($P = 0.04$).

Finally, we assessed the associations of conventional prognostic markers, such as incomplete resection, Hyams grade, Dulguerov T stage, and Kadish stage, with survival. As shown in Figure S3, only surgical margins and the Hyams grade were statistically associated with survival; however, in our series, the difference was less significant than when the CD4/CD8 ratio or Ki67 PI was used.

Discussion

This work was conducted in order to attempt to highlight new prognostic markers and help physicians with their treatment decisions. Whereas some studies suggest that the clinical stage is the best prognostic parameter,[24] others recommend histological grading.[3,13] It is probable that both clinical stage and histological grade need to be taken into account in the final therapeutic decision. However, the Hyams histological grade is questionable, especially in grade III cases. Malouf *et al.* suggested that the grade III category be divided into two categories, i.e. 'I–II' and 'III–IV'.[14] As ONBs share many characteristics with neuroendocrine tumours, and as the Ki67 PI is widely used as a prognostic marker in these entities, the idea of adding the Ki67 PI to the Hyams grade is already under consideration by pathologists.[17] Singh *et al.* reported a Ki67 PI of >25 to be a significant

Table 4. Stromal and intratumoral TILs according to low or high Hyams grade

	Median (cell/mm^2) ± MAD		
	Hyams I–II	Hyams III–IV	*P*-value
Stromal CD20+ TILs	108.5 ± 96 (n = 28)	59 ± 36 (n = 17)	0.3430
Intratumoral CD20+ TILs	0 ± 0 (n = 28)	0 ± 0 (n = 17)	0.7802
Stromal CD4+ TILs	177.5 ± 116 (n = 28)	316 ± 161 (n = 17)	0.1466
Intratumoral CD4+ TILs	14 ± 10.5 (n = 28)	62 ± 51 (n = 17)	**0.0068**
Stromal CD8+ TILs	171 ± 82.5 (n = 28)	240 ± 84 (n = 17)	**0.0246**
Intratumoral CD8+ TILs	5.5 ± 5.5 (n = 28)	37 ± 26 (n = 17)	**0.0026**

Significant differences are in bold.
MAD, Median absolute deviation; TILs, Tumour-infiltrating lymphocytes.

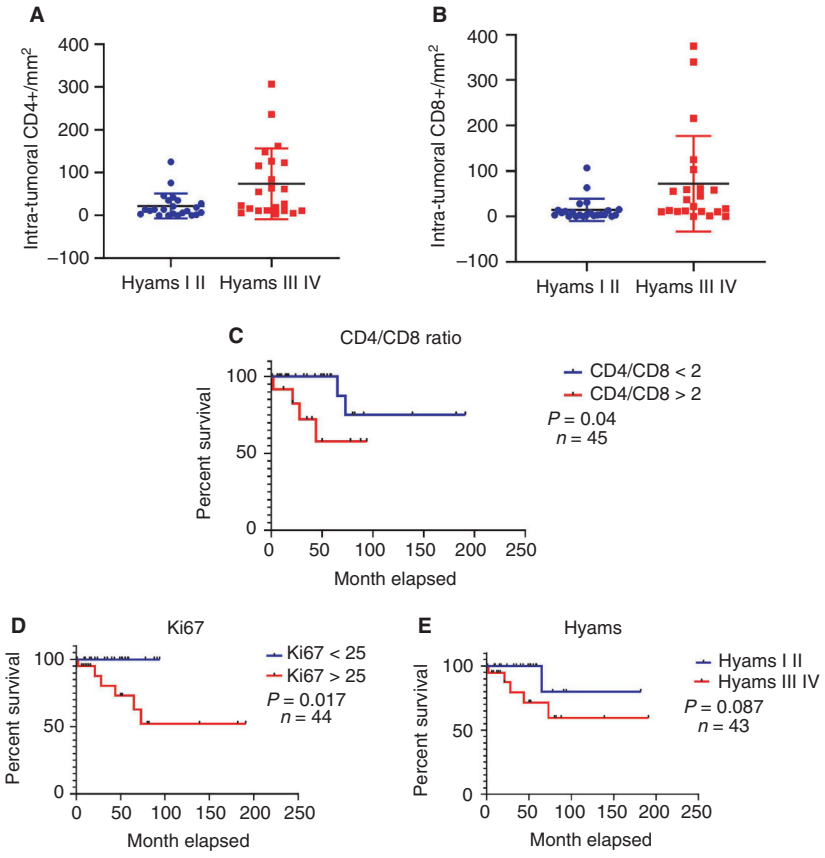

Figure 5. Differences in tumour-infiltrating lymphocyte distribution between low-grade and high-grade olfactory neuroblastomas (ONBs), and survival curve, according to the CD4/CD8 ratio. **A**, Scatterplot of intratumoral CD4+ cells between Hyams I–II and Hyams III–IV ONBs, showing a significantly larger number of CD4+ T cells in high-grade ONBs; the error bars represent the mean and the standard deviation. **B**, Scatterplot of intratumoral CD8+ cells between Hyams I–II and Hyams III–IV ONBs, showing a significantly larger number of CD4+ T cells in high-grade ONBs; the error bars represent the mean and the standard deviation. **C**, Overall survival according to the CD4/CD8 ratio with 2 as a threshold; cases showing a CD4/CD8 ratio of >2 had significantly shorter survival. **D**, Overall survival according to the Ki67 proliferation index (PI) with 25 as a threshold; cases showing a Ki67 PI of ≥25 had significantly shorter survival. **E**, Overall survival according to the Hyams grade, separating Hyams I–II from Hyams III–IV cases; cases showing a Hyams grade evaluated as III–IV tended to have shorter survival, but the difference was not significant. [Colour figure can be viewed at wileyonlinelibrary.com]

prognostic marker among a series of 26 ONBs.[18] In our study's 45 cases, 25 was the highest Ki67 PI observed among low-grade ONBs. We confirmed that a Ki67 PI of ≥25 was predictive of poorer survival. This could be the start of an update of the Hyams grading system, if confirmed by others.

The biology of tumours is no longer the only factor to be taken into account in the case of cancers. The tumour microenvironment and, especially, the immune environment impact on therapeutic strategies are important, as shown over the past few years with the advent of immune-modulating therapies.[25–27] TILs have been studied in several cancers, but never in ONB. Here, for the first time, we describe TILs in this entity. To understand the potential role of TILs in the prognosis of ONBs, we studied the effect of TILs, as well as the effects of more conventional and validated prognostic criteria, on survival. The number of TILs was variable among the cases (from 37 to 3120 cells/mm^2 for CD4+), but, with a median of 301 CD4+ cells/mm^2 and 227 CD8+ cells/mm^2, we showed that some ONBs are significantly infiltrated by immune cells and can be considered to be 'hot' tumours. We found that CD4+ or CD8+ infiltration did not impact on survival, but that a CD4/CD8 ratio of >2 was associated with poorer prognoses. This suggests that the balance between CD4+ and CD8+ T cells is more important than the absolute number of TILs, and that a higher proportion of CD4+ cells than CD8+ cells is associated with a poorer prognosis. The CD4/CD8 ratio has already been reported as a prognostic marker in human papillomavirus (HPV)-related

laryngeal squamous cell carcinomas, with the CD4/CD8 ratio being lower in HPV-positive than in HPV-negative cases, showing that HPV-positive cancers are better prognostic markers.[28] In our case, at least some of the CD4+ cells composing the infiltrate might be regulatory T cells (Tregs). This could explain the unfavourable impact of a high CD4/CD8 ratio. Sato *et al.* reported that a high CD8+ cell/Treg ratio was associated with a favourable prognosis in ovarian cancer.[29] They noted that the unfavourable effect of CD4+ T cells on prognosis was due to FOXP3+ regulatory T cells. This might be the case for ONBs too. A high number of Tregs has also been reported as a marker of poor prognosis,[30,31] notably in pancreatic ductal adenocarcinoma,[32] hepatocellular carcinoma,[33,34] and breast carcinoma.[35] The prognostic significance of TILs has now been shown in many cancers, predominantly in colorectal carcinoma cases associated with microsatellite instability (MSI).[36] The favourable prognostic impact of immunity in tumours with MSI could be due to a high mutational load.[36,37] Our results show that high-grade ONBs are highly infiltrated by TILs, and that high-grade tumours show more CD8+ cells ($P = 0.015$) and CD4+ cells ($P = 0.043$) than low-grade cases. This might be due to the stronger immunogenic profile of high-grade tumours. The mutational landscape of ONBs is still poorly known.[38–40] Classe *et al.* reported different mutational profiles in low-grade and high-grade ONBs, with no recurrent mutations in low-grade ONBs, and *IDH2* and *TP53* mutations in higher-grade ONBs. *TP53* mutations have also been reported by others in high grade ONBs.[38–40] It is possible that high-grade tumours have a higher mutational load than low-grade tumours, or have mutations that are more immunogenic.

Unlike T cells, B cells were found to be restricted to the stromal compartment of the tumour. However, despite the reported role of B cells in anticancer immune responses,[41–43] we found no association between B-cell infiltration and grade or prognosis in ONBs. Castino *et al.* reported that the prognostic influence of B cells was associated with tertiary lymphoid structures.[41] As most of our samples were obtained from endoscopic surgery, the invasion border was hardly available, owing to surgical sampling, and we observed no tertiary lymphoid structures. This might explain why we found no impact of B cells on prognosis in our samples.

In order to evaluate the effects of TILs and the Ki67 PI on survival, we also studied other, more conventional, prognostic markers in the same cohort. Like other studies, we found that a high Hyams grade[10,14,44] tended to be associated with poorer survival ($P = 0.09$) (Figure 5E). We also highlighted the unfavourable effect of incomplete surgical resection, which had, to our knowledge, not been reported before. Recently, in a large series of 187 ONBs, it was reported that, although no standard treatment exists for ONB, the therapeutic strategy would have an important prognostic role.[45] In our series, the therapeutic strategies were not homogeneous; therefore, we did not evaluate the impact of the different treatment combinations.

In summary, we have shown that Ki67 proliferation was significantly higher in high-grade ONBs, and that a Ki67 PI of ≥25 was associated with poorer survival. We also have demonstrated that high-grade ONBs show more intratumoral TILs than low-grade ONBs. Our work suggests that the CD4/CD8 ratio could also represent an interesting prognostic marker. With 45 cases and a mean follow-up of 46 months, even if the therapeutic strategies were not always homogeneous among the patients, this series confirms the importance of histological grading, and suggests that the Ki67 PI could become an objective prognostic marker in these tumours. Our study also shows the importance of immune responses in ONBs, suggesting that a careful evaluation of TILs could prove to be a powerful prognostic tool for identifying patients with distinct clinical behaviours and responses to immunotherapeutic strategies.

Acknowledgements

The authors want to thank Professsor Homa Adle Biassette and the Lariboisière Biological Resources Centre.

Conflict of interest

The authors have no conflicts of interest or funding to disclose.

Author contributions

Conceptualization: M. Classe, A. Burgess, G. G. Malouf, and B. Verillaud. Methodology and investigation: M. Classe, B. Verillaud, M. Wassef, G. G. Malouf, A. Burgess, and B. Verillaud. Formal analysis: M. Classe, A. Burgess, G. G. Malouf, and B. Verillaud. Resources: P. Herman, G. Mortuaire, X. Leroy, M. Wassef, and S. El Zein. Writing, review, and editing: M. Classe, A. Burgess, and B. Verillaud.

Ethical approval

This study was performed according to the Declaration of Helsinki. It was a retrospective study using pre-existing specimens, so written consent was not required.

References

1. Bell DFA, Gillison M, Thompson LDR, Wenig BM. Tumours of the nasal cavity, paranasal sinuses and skull base. In El-Naggar AK, Chan JKC, Grandis JR, Takata T, Slootweg PJ eds. *World Health Organization classification of head and neck tumours*. Lyon: IARC Press, 2017; 57–59.
2. Thompson LD. Olfactory neuroblastoma. *Head Neck Pathol.* 2009; **3**; 252–259.
3. Saade RE, Hanna EY, Bell D. Prognosis and biology in esthesioneuroblastoma: the emerging role of Hyams grading system. *Curr. Oncol. Rep.* 2015; **17**; 423.
4. Bell D, Hanna EY, Weber RS *et al*. Neuroendocrine neoplasms of the sinonasal region. *Head Neck* 2016; **38**(Suppl. 1); E2259–E2266.
5. Faragalla H, Weinreb I. Olfactory neuroblastoma: a review and update. *Adv. Anat. Pathol.* 2009; **16**; 322–331.
6. Thompson LD. Small round blue cell tumors of the sinonasal tract: a differential diagnosis approach. *Mod. Pathol.* 2017; **30**; S1–S26.
7. Su SY, Bell D, Hanna EY. Esthesioneuroblastoma, neuroendocrine carcinoma, and sinonasal undifferentiated carcinoma: differentiation in diagnosis and treatment. *Int. Arch. Otorhinolaryngol.* 2014; **18**; S149–S156.
8. Ow TJ, Bell D, Kupferman ME, Demonte F, Hanna EY. Esthesioneuroblastoma. *Neurosurg. Clin. North Am.* 2013; **24**; 51–65.
9. Dulguerov P, Calcaterra T. Esthesioneuroblastoma: the UCLA experience 1970–1990. *Laryngoscope* 1992; **102**; 843–849.
10. Dulguerov P, Allal AS, Calcaterra TC. Esthesioneuroblastoma: a meta-analysis and review. *Lancet Oncol.* 2001; **2**; 683–690.
11. Morita A, Ebersold MJ, Olsen KD, Foote RL, Lewis JE, Quast LM. Esthesioneuroblastoma: prognosis and management. *Neurosurgery* 1993; **32**; 706–714; discussion 714–715.
12. Gallagher KK, Spector ME, Pepper JP, McKean EL, Marentette LJ, McHugh JB. Esthesioneuroblastoma: updating histologic grading as it relates to prognosis. *Ann. Otol. Rhinol. Laryngol.* 2014; **123**; 353–358.
13. Bell D, Saade R, Roberts D *et al*. Prognostic utility of Hyams histological grading and Kadish-Morita staging systems for esthesioneuroblastoma outcomes. *Head Neck Pathol.* 2015; **9**; 51–59.
14. Malouf GG, Casiraghi O, Deutsch E, Guigay J, Temam S, Bourhis J. Low- and high-grade esthesioneuroblastomas display a distinct natural history and outcome. *Eur. J. Cancer* 2013; **49**; 1324–1334.
15. Kaur G, Kane AJ, Sughrue ME *et al*. The prognostic implications of Hyam's subtype for patients with Kadish stage C esthesioneuroblastoma. *J. Clin. Neurosci.* 2013; **20**; 281–286.
16. Matsukuma K, Olson KA, Gui D, Gandour-Edwards R, Li Y, Beckett L. Synaptophysin–Ki67 double stain: a novel technique that improves interobserver agreement in the grading of well-differentiated gastrointestinal neuroendocrine tumors. *Mod. Pathol.* 2017; **30**; 620–629.
17. Hirose T, Scheithauer BW, Lopes MB *et al*. Olfactory neuroblastoma. An immunohistochemical, ultrastructural, and flow cytometric study. *Cancer* 1995; **76**; 4–19.
18. Singh L, Ranjan R, Madan R, Arava SK, Deepak RK, Singh MK. Microvessel density and Ki-67 labeling index in esthesioneuroblastoma: is there a prognostic role? *Ann. Diagn. Pathol.* 2015; **19**; 391–396.
19. Kirilovsky A, Marliot F, El Sissy C, Haicheur N, Galon J, Pages F. Rational bases for the use of the immunoscore in routine clinical settings as a prognostic and predictive biomarker in cancer patients. *Int. Immunol.* 2016; **28**; 373–382.
20. Mlecnik B, Bindea G, Kirilovsky A *et al*. The tumor microenvironment and immunoscore are critical determinants of dissemination to distant metastasis. *Sci. Transl. Med.* 2016; **8**; 327ra326.
21. Mlecnik B, Bindea G, Angell HK *et al*. Integrative analyses of colorectal cancer show immunoscore is a stronger predictor of patient survival than microsatellite instability. *Immunity* 2016; **44**; 698–711.
22. Schoenfeld JD. Immunity in head and neck cancer. *Cancer Immunol. Res.* 2015; **3**; 12–17.
23. Nguyen N, Bellile E, Thomas D *et al*. Tumor infiltrating lymphocytes and survival in patients with head and neck squamous cell carcinoma. *Head Neck* 2016; **38**; 1074–1084.
24. Tajudeen BA, Arshi A, Suh JD *et al*. Esthesioneuroblastoma: an update on the UCLA experience, 2002–2013. *J. Neurol. Surg. B Skull Base* 2015; **76**; 43–49.
25. Becht E, Giraldo NA, Dieu-Nosjean MC, Sautes-Fridman C, Fridman WH. Cancer immune contexture and immunotherapy. *Curr. Opin. Immunol.* 2016; **39**; 7–13.
26. Fridman WH, Pages F, Sautes-Fridman C, Galon J. The immune contexture in human tumours: impact on clinical outcome. *Nat. Rev. Cancer* 2012; **12**; 298–306.
27. Xie X, O'Neill W, Pan Q. Immunotherapy for head and neck cancer: the future of treatment? *Expert Opin. Biol. Ther.* 2017; **17**; 701–708.
28. Zhang D, Tang WJ, Tang D *et al*. The ratio of CD4/CD8 T-cells in human papillomavirus-positive laryngeal squamous cell carcinoma accounts for improved outcome. *Acta Otolaryngol.* 2016; **136**; 826–833.
29. Sato E, Olson SH, Ahn J *et al*. Intraepithelial CD8+ tumor-infiltrating lymphocytes and a high CD8+/regulatory T cell ratio are associated with favorable prognosis in ovarian cancer. *Proc. Natl Acad. Sci. USA* 2005; **102**; 18538–18543.
30. Chaudhary B, Elkord E. Regulatory T cells in the tumor microenvironment and cancer progression: role and therapeutic targeting. *Vaccines (Basel)* 2016; **4**; 28.
31. De Meulenaere A, Vermassen T, Aspeslagh S, Vandecasteele K, Rottey S, Ferdinande L. TILs in head and neck cancer: ready for clinical implementation and why (not)? *Head Neck Pathol.* 2016; **11**; 354–363.
32. Hiraoka N, Onozato K, Kosuge T, Hirohashi S. Prevalence of FOXP3+ regulatory T cells increases during the progression of pancreatic ductal adenocarcinoma and its premalignant lesions. *Clin. Cancer Res.* 2006; **12**; 5423–5434.
33. Fu J, Xu D, Liu Z *et al*. Increased regulatory T cells correlate with CD8 T-cell impairment and poor survival in hepatocellular carcinoma patients. *Gastroenterology* 2007; **132**; 2328–2339.
34. Sasaki A, Tanaka F, Mimori K *et al*. Prognostic value of tumor-infiltrating FOXP3+ regulatory T cells in patients with hepatocellular carcinoma. *Eur. J. Surg. Oncol.* 2008; **34**; 173–179.

35. Merlo A, Casalini P, Carcangiu ML *et al*. FOXP3 expression and overall survival in breast cancer. *J. Clin. Oncol.* 2009; **27**; 1746–1752.
36. Basile D, Garattini SK, Bonotto M *et al*. Immunotherapy for colorectal cancer: where are we heading? *Expert Opin. Biol. Ther.* 2017; **17**; 1–13.
37. Le DT, Uram JN, Wang H *et al*. PD-1 blockade in tumors with mismatch-repair deficiency. *N. Engl. J. Med.* 2015; **372**; 2509–2520.
38. Gay LM, Kim S, Fedorchak K *et al*. Comprehensive genomic profiling of esthesioneuroblastoma reveals additional treatment options. *Oncologist* 2017; **22**; 834–842.
39. Lazo de la Vega L, McHugh JB, Cani AK *et al*. Comprehensive molecular profiling of olfactory neuroblastoma identifies potentially targetable FGFR3 amplifications. *Mol. Cancer Res.* 2017; **15**; 1551–1557.
40. Classe M, Yao H, Mouawad R *et al*. Integrated multi-omic analysis of esthesioneuroblastomas identifies two subgroups linked to cell ontogeny. *Cell Rep.* 2018; **25**; 811–821.
41. Castino GF, Cortese N, Capretti G *et al*. Spatial distribution of B cells predicts prognosis in human pancreatic adenocarcinoma. *Oncoimmunology* 2016; **5**; e1085147.
42. Linnebacher M. Tumor-infiltrating B cells come into vogue. *World J. Gastroenterol.* 2013; **19**; 8–11.
43. Knief J, Reddemann K, Petrova E, Herhahn T, Wellner U, Thorns C. High density of tumor-infiltrating B-lymphocytes and plasma cells signifies prolonged overall survival in adenocarcinoma of the esophagogastric junction. *Anticancer Res.* 2016; **36**; 5339–5345.
44. Van Gompel JJ, Giannini C, Olsen KD *et al*. Long-term outcome of esthesioneuroblastoma: Hyams grade predicts patient survival. *J. Neurol. Surg. B Skull Base* 2012; **73**; 331–336.
45. Xiong L, Zeng XL, Guo CK, Liu AW, Huang L. Optimal treatment and prognostic factors for esthesioneuroblastoma: retrospective analysis of 187 Chinese patients. *BMC Cancer* 2017; **17**; 254.

Supporting Information

Additional Supporting Information may be found in the online version of this article:

Figure S1. Point cloud showing the correlation between the Ki67 PI and the mitotic count in ONBs.

Figure S2. Distribution of the CD4/CD8 ratio among the samples.

Figure S3. Survival curves according to the different prognostic factors studied.

Table S1. Immunohistochemistry references and protocols.

Table S2. Ki67 ROC curve data.

Table S3. Descriptive statistics for parameter mitoses/2.5 mm^2.

Table S4. Correlation matrix corresponding to Figure S2 (TIL parameters, Ki67 PI, and mitotic count).